Ceramic papers containing Y zeolite for toluene removal

Juan Pablo Cecchini [a], Ramiro M. Serra [a], César M. Barrientos [a,b], María A. Ulla [a], María V. Galván [b], Viviana G. Milt [a,*]

[a] Instituto de Investigaciones en Catálisis y Petroquímica (INCAPE, FIQ-UNL-CONICET), Santiago del Estero 2829, 3000 Santa Fe, Argentina
[b] Instituto de Tecnología Celulósica, FIQ, UNL, Santiago del Estero 2564, Santa Fe, S3000 AOJ, Argentina

ARTICLE INFO

ABSTRACT

A papermaking technique with a dual polyelectrolyte retention system was used for the preparation of NaY zeolite-containing papers, which implied the use of cationic and anionic polymers. Two kinds of fibers were employed, either cellulosic or ceramic ones, and accordingly papers with different characteristics were obtained: those that only contained cellulosic fibers for low temperature applications, cellulosic papers, and those prepared using both cellulosic and ceramic fibers – ceramic papers – for high temperature applications. Although a decrease in their mechanical properties due to calcination was observed, zeolitic ceramic papers resulted easy to handle for practical applications.

Zeolite was quantified through BET surface area measurements. SEM images indicated a good dispersion of zeolite particles within the cellulosic paper whereas in the ceramic paper they appeared anchored on ceramic fibers.

The zeolitic papers prepared resulted efficient as toluene sorbents, the adsorption capacities of zeolitic ceramic papers being higher than those of zeolitic cellulosic papers. In the case of zeolitic cellulosic papers, the amounts of released toluene were lower than those of adsorbed toluene, implying that the treatment up to 160 °C did not completely eliminate the hydrocarbon. Also, TPD profiles showed that toluene is chemically retained up to high temperatures (ca. 420 °C) in zeolitic ceramic papers.

Toluene adsorption values demonstrate that zeolite dispersed into the cellulose/ceramic matrix is as effective as powder massive zeolite in retaining the hydrocarbon, which highlights the potential application of these zeolitic structures as sorbent materials both for low and high temperatures.

Published by Elsevier Inc.

1. Introduction

Volatile organic compounds (VOCs) vaporize easily at low temperatures and include most thinners, solvents, degreasers, cleaners, lubricants and liquid fuels. The most common VOCs include acetaldehyde, acetone, benzene, ethyl acetate, carbon tetrachloride, ethylene glycol, formaldehyde, heptane, hexane, isopropyl alcohol, methyl ethyl ketone, methyl chloride, monomethyl ether, naphthalene, toluene and xylene. VOCs pollutants can come from indoor and outdoor sources. Indoor VOCs pollution often originates from household products such as office supplies, insulating materials, cleaning products, and pressed woods, or may originate from tobacco smoke [1]. On the other hand, outdoor VOCs pollution is mainly originated from emissions of industrial processes and automobile exhausts. From the environmental point of view, it is necessary to limit and control vapor emissions, which affect climate change, the growth and decay of plants, and the health of humans and animals [2,3].

Toluene is a typical indoor pollutant and its discharge may produce irritation of the eyes and the respiratory tract, nausea, headache, fatigue, dullness and thirst, even at very low concentrations [4,5]. Using gaseous air cleaners in non-industrial buildings also has the potential to save money by reducing sick building syndrome symptoms and improving work productivity [6].

During the last decades the chemical industry has shown a strong interest in developing clean and sustainable technologies [2]. The analysis of the applications of fiber materials for the chemical process industry to reduce polluting emissions shows that fiber catalysts have received considerable theoretical and experimental attention. These flexible materials have the advantage of being adaptable to different geometries, allow the regulation of permeability, are effective supports for the deposition of catalysts and can be applied in a wide range of temperatures [7]. An attractive approach for the preparation of a soft membrane with adsorption properties is the combination of molecular sieve porous materials (like zeolites) with a cheap and abundant organic matrix, such as natural cellulose. Once a stable zeolite/cellulose material is synthesized, paper filters can be obtained, and when thermal resistance is

required, ceramic fibers can be used in combination with cellulose ones [4,8–10].

In this context, the main objective of this work is the preparation of Y zeolite-containing papers, their characterization and the evaluation of their performances as adsorbents for VOCs using toluene as a representative molecule. In order to extend the operation temperature range of the zeolite papers, the use of ceramic fibers along with cellulose ones was explored.

2. Experimental

2.1. Ceramic paper preparation

In order to obtain the zeolitic ceramic paper, two kinds of fibers were used: ceramic fibers (50 wt.% SiO_2, 48 wt.% Al_2O_3 and 2 wt.% impurities), obtained from a ceramic cloth from CARBO by elutriation, and cellulosic fibers obtained by repulping an industrial blotting paper produced from virgin softwood Kraft slightly-refined fibers. Ceramic fibers have an average length of 660 μm and an average diameter of 6 μm, whereas cellulosic fibers are 3 mm long and have a ribbon shape with an average width of 30 μm.

A papermaking technique with a dual polyelectrolyte retention system was used for which cationic and anionic polymers were employed. The cationic polymer was polyvinyl amine (PVAm) (Luredur PR 8095) from BASF, molecular weight 4×10^5 g/mol and charge density 4.5 meq/g and the anionic polymer was anionic polyacrylamide (A-PAM) from AQUATEC, molecular weight 10^4–10^5 g/mol and charge density 2.7 meq/g. Commercial NaY zeolite from Linde, Si/Al ratio equal to 3.5, was employed.

NaY zeolite (3.5 g) was added to a 500 ml solution volume of NaCl solution (0.01 N). Under soft agitation, 3.5 g of ceramic fiber, 3.5 g of cellulose and 33 ml PVAm solution (9 g/l) were incorporated. After 3 min of agitation, 21 ml A-PAM polymer solution (0.39 g/l) was added. With this suspension, a sheet was structured by the SCAN standard method [11] using water of 180 mS of conductivity and applying the double of the usual pressing pressure. The wet sheet was dried at 105 °C during 24 h and finally calcined in air for 2 h at 600 °C. The paper thus formed was called zeolitic ceramic paper, "PCer Z".

Following the same procedure other papers were prepared: A paper with all the above-mentioned ingredients but without the addition of zeolite, called "PCer", a paper with all the above-mentioned ingredients but replacing ceramic by cellulose fibers, called "PCel Z" and a cellulose paper (replacing ceramic by cellulose fibers and without zeolite) denominated as "PCel". Fig. 1 schematizes the preparation procedure. It is important to

remark that papers denoted as "PCer" and "PCer Z" (ceramic papers) were calcined at 600 °C but those denoted as "PCel Z" and "PCel" (cellulosic papers) were only air-dried under papermaking standard conditions (23 °C-50%RH).

2.2. Physicochemical and mechanical characterizations

2.2.1. Airflow resistance

The sheet porosity was evaluated by determining the air resistance of the catalytic papers by measuring the time for a given volume of air to flow through the sheet. For this purpose, a Gurley-Hill, SPS tester was used.

2.2.2. Tensile strength

An INSTRON 3344 universal tester, with reference standard TAPPI T494-01 om was used.

2.2.3. Optical microscopy

The morphological aspects of the papers were examined using a Leica Stereozoom DM500 stereomicroscope.

2.2.4. Scanning electron microscopy (SEM)

A SEM Jeol JSM-35C equipment was employed operated at 20 kV acceleration voltage. Samples were glued to the sample holder with Ag painting and then coated with a thin layer of Au in order to improve the images.

2.2.5. XRD characterization

Crystalline phases were determined with a Shimadzu XD-D1 instrument with monochromator using Cu Kα radiation at a scan rate of 1°/min, from $2\theta = 5°$ to 50°. The pieces of about 2 cm × 2 cm were supported in a special sample holder designed for the XRD analysis. The software package of the equipment was used for the phase identification from the X-ray diffractograms.

2.2.6. TGA–SDTA

The thermal behavior of the ceramic papers was studied in a Mettler Toledo TGA/SDTA 851 instrument. The weight changes and the differential thermal process of the catalytic ceramic papers (10 mg of samples) were analyzed from 25 to 1000 °C with a heating rate of 10 °C/min in air flow (80 ml/min).

2.2.7. Textural properties

Nitrogen adsorption–desorption isotherms were obtained at −196 °C on a Quantachrome Autosorb 1C instrument. Previously, samples were outgassed at 105 °C for 2 h under vacuum. The
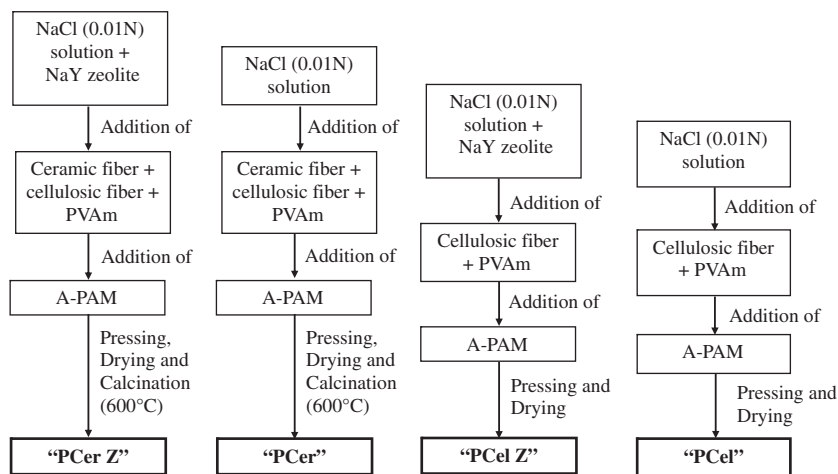

Fig. 1. Scheme of the catalytic paper preparation.

Brunauer–Emmett–Teller (BET) equation was used for calculating the specific surface area of the materials from nitrogen adsorption isotherms.

2.3. Toluene adsorption and desorption

The breakthrough curves and temperature-programmed desorption profiles were obtained using a continuous flow system and toluene as probe molecule representative of cyclic hydrocarbons present in VOCs emissions.

2.3.1. Cellulosic papers

150 mg of the cellulosic paper (either "PCel Z" or "PCel") were tightly rolled on and put into a tubular quartz reactor (5 mm i.d.). Then, He flow (40 cm^3/min) was passed and the paper was heated up to 160 °C at 10 °C/min, maintaining this temperature for 1 h. Then, under He flow, the paper was cooled down to the adsorption temperature (50 or 100 °C). After stabilization of the adsorption temperature, a stream of toluene diluted in He (40 cm^3/min) was passed through the paper bed during 40 min. The toluene stream was achieved by passing He flow through two saturators containing toluene (99.9%, Sigma–Aldrich) immersed in an ice bath so that the initial concentration was about 8000 ppm of toluene in the He stream. After saturation, He flow was passed during 15 min for toluene removal and the TPD experiment was carried out under He flow, heating from the adsorption temperature to 160 °C at 10 °C/min and maintaining this temperature up to complete toluene removal or until achieving constant toluene concentration, which was continuously monitored ($m/e = 91$) by on-line mass spectroscopy (Pfeiffer/Balzers Quadstar, QMI422, QME125).

2.3.2. Ceramic papers

60 mg of the ceramic paper (either "PCer Z" or "PCer") was tightly rolled on and put into the tubular quartz reactor (above described) and pretreated under He flow (40 cm^3/min) at 400 °C for 1 h. Then, still under He flow, the paper was cooled down to the adsorption temperature (100 °C) and after stabilization of this temperature, a stream of toluene diluted in He (40 cm^3/min) was passed through the paper bed during 40 min. After saturation, He flow was passed during 15 min and the TPD experiment was carried out under He flow, heating from 100 °C to 550 °C at 10 °C/min and maintaining this temperature up to complete toluene removal. As above described, toluene was continuously monitored ($m/e = 91$) by on-line mass spectroscopy. In order to assure that toluene did not decompose under TPD conditions, $m/e = 14$, 15 and 44 were also monitored.

2.3.3. Quantification

The toluene adsorption capacity was calculated from the breakthrough curves as the difference between the area under the curve in a blank experiment and the area under the breakthrough profile. The amount of retained toluene after the He purge was calculated as the area under the TPD peak during the heating treatment. In the case of the cellulosic paper, the area under the curve was used for calculations since no defined TPD peak was obtained after heating up to 160 °C.

3. Results and discussion

3.1. Mechanical tests

Cellulose can be considered a polyvalent alcohol, with three unbound OH groups contained in each structural unit that form intrafiber and interfiber hydrogen bonds, which is reflected in

Table 1
Mechanical tests.

SAMPLE	Air flow resistance (seg/100 ml)	Tensile strength (Nm/g)
"PCel"	19.1	38.5
"PCel Z"	15.7	10.7
"PCer"[*]	1.9	13.5
"PCer Z"[*]	0.8	3.9

[*] Before calcination.

the paper strength. In order to study the effect of both the partial replacement of cellulosic fibers by ceramic fibers and the influence of zeolite on the quality of the paper, flow resistance and tensile strength tests were performed on uncalcined papers (Table 1). It can be noticed that "PCel" was much more resistant to airflow (approximately 10 times) and is stronger (approximately three times) than the "PCer". As reported, ceramic fibers have no ability to form interfiber bonds, not contributing to paper strength or airflow resistance, either [12].

The addition of Y zeolite to the papers reduced the airflow resistance, having a significant impact on the "PCer Z". In this case, the decrease to the airflow resistance was 58%, whereas the airflow resistance only decreased 18% when comparing "PCel Z" and "PCel". There was also a significant decrease in the values of tensile strength: approximately 70% less tensile strength exhibited the zeolite-containing papers when compared with those without zeolite. This effect could be due to the influence of the zeolite structure that would reduce the contact area between the fibers. Nevertheless, zeolite particles did not inhibit cellulose fiber-to-fiber contact.

Even though the air flow resistance and the tensile strength are lower for the ceramic papers (PCer Z and PCer) than for the cellulose papers (PCel or PCel Z), values belonging to the formers are good enough for practical applications. Ceramic papers thus obtained are easy to handle in practical use and allow ceramic papers to be rolled and folded without breaking.

3.2. Papers morphology

Fig. 2a shows a picture of the "PCel Z" sample observed by an optical microscope. The fibers observed correspond to cellulose and bright particles (of about 20 μm in diameter) distributed all along the surface and correspond to Y zeolite (indicated by circles), which has been inserted and retained into the fibrous matrix by effect of the polyelectrolytes.

Fig. 2b shows an image obtained for the "PCer Z" sample before calcination using the optical microscope, where a combination of cellulosic and ceramic fibers (indicated by arrows) and zeolite particles is observed. Cellulosic and ceramic fibers appear forming characteristic network structures and zeolite particles are homogenously distributed on the sheet and impregnate all the paper thickness (not shown in Fig. 2).

In order to better examine the papers morphology and to study the effect of calcination of the ceramic paper on its structure, SEM studies were performed. Fig. 3 shows the SEM pictures obtained for "PCel Z", where a general view allows appreciating the cellulose matrix with zeolite clusters. A closer view (Fig. 3b) shows in detail zeolite crystal aggregates joined by the polymers effect. In Fig. 3c zeolite crystals with smoothed edges and sizes of about 0.5–2 μm are observed.

Fig. 4 shows the SEM pictures obtained for "PCer Z". The general view (Fig. 4a) shows the matrix formed by the ceramic fibers, which have different diameters probably due to the fact that they are made up of either of SiO$_2$ or Al$_2$O$_3$. An open structure is obtained (as airflow resistance values of Table 1 also indicate) after
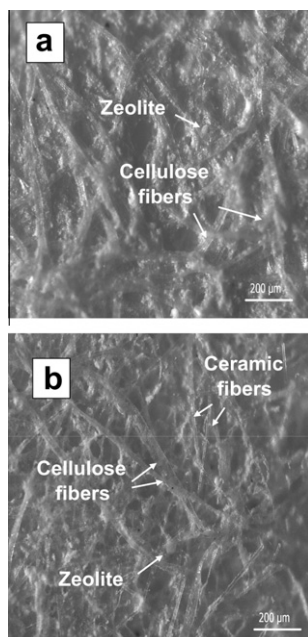
Fig. 2. Images of papers obtained by an optical microscope. (a) "PCel Z" and (b) uncalcined "PCer Z".

the calcination of the ceramic paper and zeolite groups appear attached to ceramic fibers (Fig. 4b). Fig. 4c shows that zeolite crystals are smaller than those present in the cellulosic paper ("PCel Z").

3.3. X-ray diffraction

Fig. 5 shows the XRD patterns of "PCer" before and after calcination and the "PCer Z", where the diffractogram of the powder NaY zeolite incorporated to the papers is also included for comparison. Wide peaks observed at ca. 15.7° and 22.5° for "PCer" before calcination correspond to crystalline cellulose [13] and although this paper contains ceramic fibers, no signals

associated with either Al_2O_3 or SiO_2 are observed. However, cellulose signals appear mounted over an amorphous halo, more clearly observed when "PCer" is calcined up to 600 °C ("PCer" profile). As observed, cellulose is completely destroyed after calcination at 600 °C. The "PCer Z" sample preserves the structure of the zeolite after calcination at 600 °C for 2 h. Calcination did not destroy the zeolite structure and patterns of the NaY zeolite calcined at 600 °C (not shown) were similar to those of the fresh NaY zeolite diffractogram (upper XRD pattern of Fig. 5).

3.4. Thermal studies

The thermograms of uncalcined papers present two weight loss processes (as indicated in Fig. 6): the first one caused by elimination of water ($T < 200$ °C) and the other due to the destruction of cellulose. As expected, "PCer" shows no significant changes in weight and the weight loss observed in the "PCer Z" sample at low temperature is due to adsorbed water by the zeolite. The higher weight loss observed in the uncalcined "PCel Z" paper when compared to the uncalcined "PCer Z" paper is due to the higher proportion of cellulose in this sample [14].

The retention of inorganic materials was estimated from the ash contents of the sheets after treating the samples up to 1000 °C and referred to dry weights. The retention of inorganic materials (ceramic fiber + zeolite + ash) on "PCer Z" was about 92% and increased to 97% for "PCel Z" (retention of zeolite + ash), results that are in agreement with similar published results [15].

Fig. 7 shows DTA profiles. Peaks between 300 °C and 350 °C are related to the carbonization and oxidation of thermal decomposition products of cellulose. Peaks between ca. 415 and 480 °C could be attributed to the slow oxidation of coal.

3.5. Zeolite quantification

The zeolite content in the zeolitic cellulosic paper ("PCel Z") was estimated from BET specific surface area values (shown in Table 2) and considering the following simple equations, as suggested by
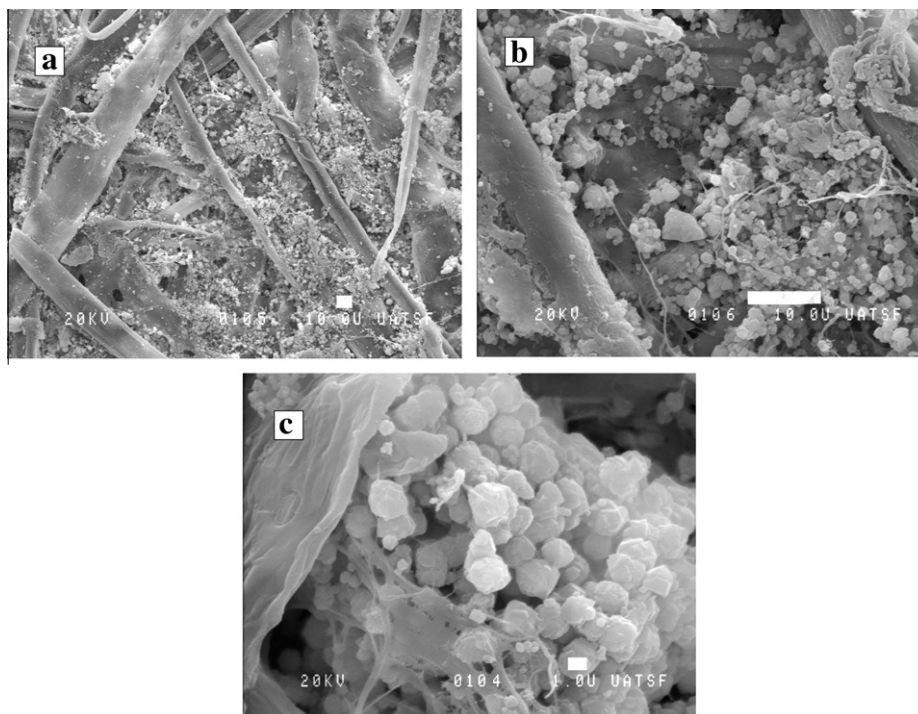

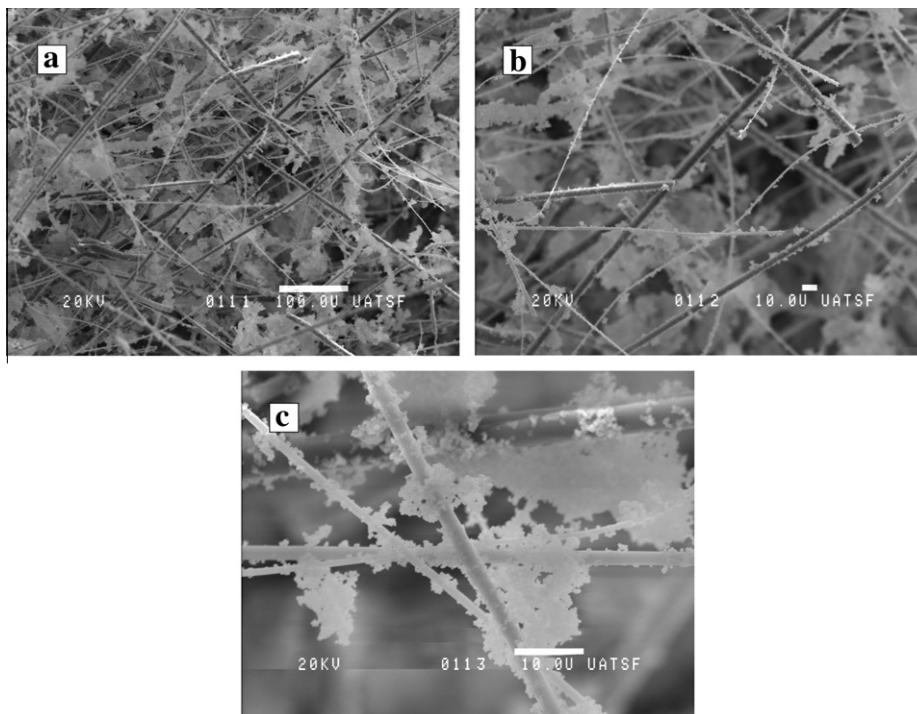**Fig. 3.** SEM images of the zeolitic cellulosic paper ("PCel Z").

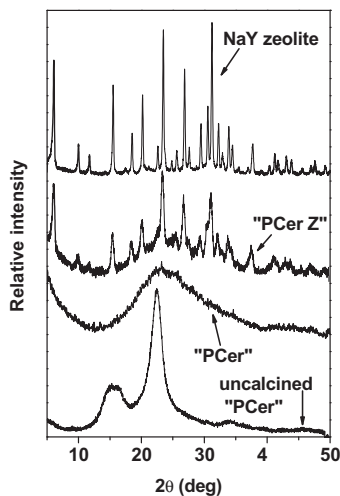**Fig. 4.** SEM images of the zeolitic ceramic paper ("PCer Z").

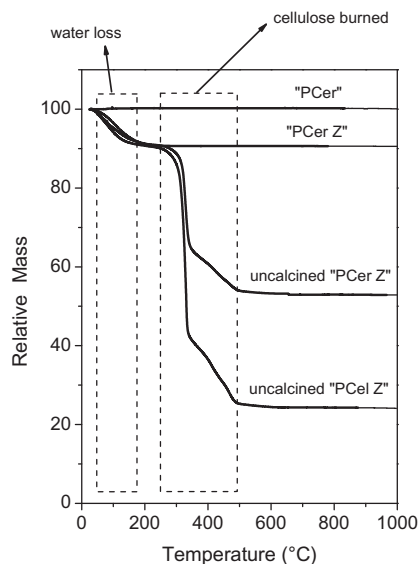**Fig. 5.** XRD diffraction patterns.

Fig. 6. Thermal behavior (TGA) of cellulosic and ceramic papers.

Vu et al. [13]: $S_{BET,PCel\ Z} = S_{BET,ZEOLITE} * X_{ZEOLITE} + S_{BET,PCel} * (1 - X_{ZEOLITE})$, where $S_{BET,PCel}$ corresponds to the BET specific surface area of the cellulosic paper, mainly constituted by cellulose fibers, and $X_{ZEOLITE}$ is the weight fraction of zeolite. Similarly, in the case of the zeolitic ceramic paper ("PCer Z"), the zeolite content was calculated from the following equation: $S_{BET,PCer\ Z} = S_{BET,ZEOLITE} * X_{ZEOLITE} + S_{BET,PCer} * (1 - X_{ZEOLITE})$, where $S_{BET,PCer}$ corresponds to the specific surface area of the ceramic fiber, which constitutes the main compound of the calcined ceramic paper without zeolite. Thus, the zeolite content determined for "PCel Z" was 28 wt.% and that corresponding to "PCer Z" was 31 wt.%.

Considering the nominal zeolite loadings during the papers manufacturing (33 wt.% zeolite for "PCel Z" and 50 wt.% for "PCer Z" that was calcined at 600 °C), the results shown in Table 2 indicate that the retention of zeolite was higher for the cellulosic

zeolitic paper, which is expected since cellulosic fibers favor particles retention due to their morphology and the functional groups they possess.

3.6. Toluene adsorption and desorption on cellulosic papers

The measurement of breakthrough curves is a direct method designed to determine the adsorption capacity of adsorbent materials. Fig. 8 shows the breakthrough curves corresponding to toluene adsorption at 50 °C and 100 °C on cellulosic papers either with or without zeolite. Bare cellulosic papers exhibit a similar toluene adsorption capacity both at 50 °C and 100 °C (0.46 µmol/mg).
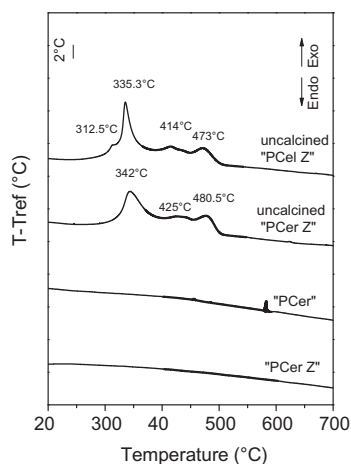
Fig. 7. SDTA profiles of ceramic and cellulosic papers.

Table 2
Zeolite quantification from BET.

Sample	BET specific surface area (S_{BET} (m²/g))	Zeolite content ($X_{ZEOLITE}$ (%))
"PCel"	1	–
"PCel Z"	193	28
"PCer Z"	235	31
Ceramic fibers	20	–
NaY zeolite	700	100

Nevertheless, the addition of zeolite notably increases the adsorption capacity of the cellulosic paper (adsorbed toluene increased from 0.46 to 7.25 μmol/mg at 50 °C and to 5.53 μmol/mg at 100 °C, Table 3), effect that could be associated with the preferential interaction of toluene with the zeolite adsorption sites. Besides, when comparing toluene adsorption both at 50 °C and 100 °C, it can be observed that the amount of adsorbed toluene decreases as temperature increases, which is a typical behavior of exothermic reversible adsorption [16].

Fig. 9 shows the TPD profiles of zeolitic cellulosic papers after adsorption at 50 °C (a) and 100 °C (b), where the maximum desorption temperature (160 °C) was selected in order to preserve
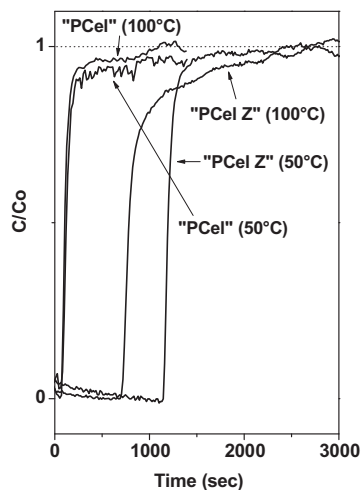

Fig. 8. Breakthrough curves of toluene adsorption onto cellulosic papers at different temperatures, 50 °C and 100 °C.

Table 3
Adsorption of toluene on zeolitic cellulosic papers ("PCel Z").

Toluene adsorption temperature (°C)	Adsorption (μmol/mg zeolite in the sample)[a]	Desorption[b] (μmol/mg zeolite in the sample)	Φ[c]
50	7.25	3.05	0.42
100	5.53	0.55	0.10

[a] Zeolite content was determined from BET measurements.
[b] Desorption values after heating the sample under He flow up to 160 °C and maintaining this temperature for 30 min.
[c] Toluene retention calculated as the ratio between desorption and adsorption (third and second columns) [18].

the cellulose structure of the paper. From Fig. 9a it is observed that the desorption of toluene begins at ca. 140 °C and the amount of desorbed hydrocarbon increases up to 160 °C. After that, toluene is gradually desorbed isothermically at 160 °C up to a constant toluene signal in the mass spectrometer is observed after 10 min. A similar behavior is observed after adsorption at 100 °C (Fig. 9b), but in this case toluene desorption begins at ca. 150 °C, the intensity of desorbed toluene is lower and 15 min are needed to observe a constant toluene signal.

Table 3 shows adsorption and desorption data of toluene, calculated as previously described in the experimental section and referred to the zeolitic content in the samples. After the treatment under He stream, the integration of the curves indicates that the retention of toluene, calculated as the ratio between desorbed and adsorbed toluene (third and second columns of Table 3), is higher after adsorption of toluene at 50 °C (0.42) than after adsorption of toluene at 100 °C (0.10).

The amounts of released toluene were lower than the adsorbed toluene amount, which implies that the treatment up to 160 °C did not allow complete toluene removal. In order to check that toluene was not completely removed after this soft treatment under inert stream up to 160 °C, a TGA experiment was performed. The paper ("PCel Z") after toluene adsorption at 100 °C (Fig. 8) followed by the desorption treatment shown in Fig. 9b (denoted as "PCel Z"*) was extracted from the reactor, put into the TGA equipment and heated under air flow up to 950 °C (Fig. 10a). The weight loss up to 330 °C was the same both for "PCel Z" and "PCel Z"*, but at higher temperatures, the weight loss was higher for "PCel Z"*. Correspondingly, the SDTA profile for "PCel Z"* exhibits a higher exothermic signal at 335 °C, attributed to both cellulose and toluene burning.

3.7. Toluene adsorption and desorption on ceramic papers

Fig. 11 shows the breakthrough curves corresponding to toluene adsorption at 100 °C on ceramic papers either with or without zeolite. Also, the breakthrough curve corresponding to powder NaY zeolite is included and their shapes correspond to microporous materials adsorption [17]. As it can be observed, the ceramic paper ("PCer") rapidly saturates with the toluene stream. Besides, the time required to reach the saturation of the material with toluene is higher for "PCer Z" than for "PCer", which is related to the high adsorption capacity of the zeolite if compared with the corresponding powder NaY zeolite curve.

Table 4 shows that the toluene adsorption capacity of the "PCer" sample notably increases when zeolite is added ("PCer Z"), in agreement with the breakthrough curves shown in Fig. 11. In the case of powder NaY zeolite, the adsorbed toluene amount at 100 °C is 5.63 μmol/mg sample, value comparable to others reported for Na Mordenite [18]. Note that the adsorption value for "PCer Z" is 6.09 μmol/mg sample (expressed in terms of zeolite content in the sample, as determined by BET), comparable to that
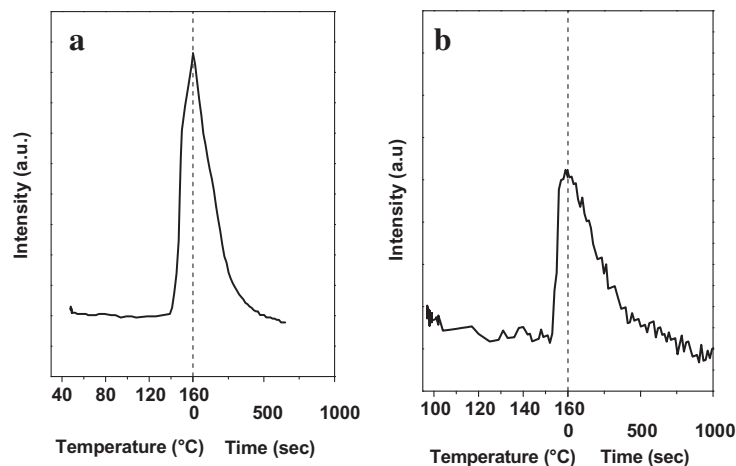
Fig. 9. Temperature-programmed desorption profiles (TPD) of adsorbed toluene on "PCel Z" after adsorption at 50 °C (a) and 100 °C (b).
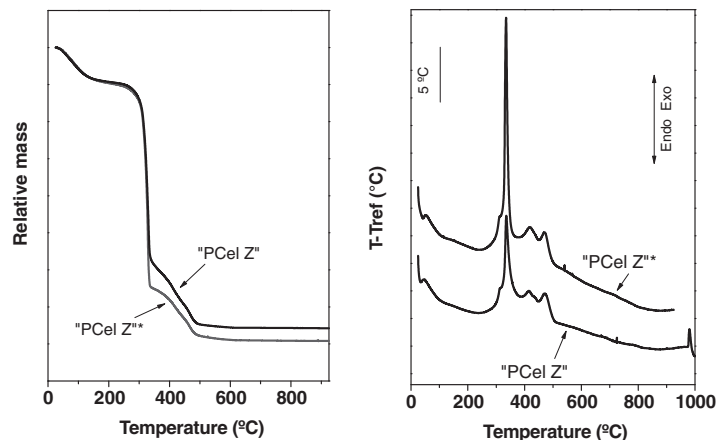

Fig. 10. Zeolitic cellulosic paper before and after the toluene adsorption and desorption experiments: (a) TGA profiles and (b) SDTA curves. "PCel Z"* indicates the zeolitic cellulosic paper extracted after the experiment shown in Fig. 9b.
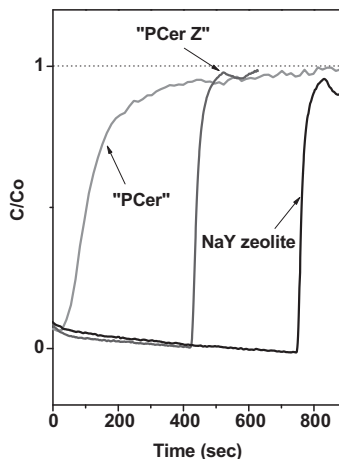

Fig. 11. Adsorption curves of toluene on different supports calcined at 600 °C.

corresponding to the powder NaY zeolite, indicating that the ceramic paper constitutes a good matrix to disperse the zeolitic material and correspondingly, "PCer Z" appears as an efficient hydrocarbon trap.

Fig. 12 shows TPD profiles corresponding to the ceramic papers and the powder NaY zeolite after adsorption at 100 °C (Fig. 11). The flat profile exhibited by the ceramic support ("PCer") indicates that toluene is mainly physisorbed in this material (Fig. 12 and Table 4), whereas the hydrocarbon is retained up to ca. 420 °C for "PCer Z". The TPD profile of "PCer Z" presents three well-defined peaks (at 228, 265 and 320 °C), which probably indicates the hydrocarbon adsorption on different sites with different adsorption energies [19]. Although the TPD profile of NaY powder zeolite shows only one peak at 294 °C, it presents three shoulders that could be associated with signals observed for "PCer Z". In both cases ("PCer Z" and NaY powder zeolite), toluene is retained up to ca. 420 °C. It is important to remark that the same adsorption–desorption profiles were obtained using different aliquots of "PCer Z". Moreover, the adsorption–desorption cycle was repeated six times over the same piece of paper and comparable breakthrough curves and TPD profiles were obtained.

The retention of hydrocarbons up to high temperatures is important for the application of these papers as sorbent materials. In this sense, Φ factors (Table 4) indicate that 20% of toluene is strongly retained for "PCer Z" (the 80% of the adsorbed toluene at 100 °C being released at low temperature, constituting physisorbed toluene) whereas ca. 40% of adsorbed toluene is strongly retained for the powder NaY zeolite.

Table 4
Adsorption and desorption toluene data of calcined samples.

SAMPLE	Adsorption[a] (μmol/mg sample)	Desorption[b] (μmol/mg sample)	Φ[c]
"PCer"	0.75	0	0
"PCer Z"	6.09[d]	1.22[d]	0.20
NaY zeolite	5.63	2.20	0.39

[a] Toluene adsorption was carried out at 100 °C.
[b] Desorption after heating up to 550 °C until complete toluene removal.
[c] Toluene retention capacity above 100 °C calculated as the ratio between desorption of toluene and the corresponding adsorption value (third and second columns) [18].
[d] In this case, adsorption is expressed in terms of zeolite content in the "PCer Z" sample, as determined by BET measurements.
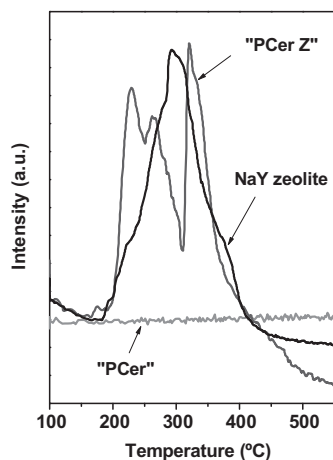

Fig. 12. Desorption curves of toluene on different supports calcined at 600 °C.

When the toluene adsorption capacities at 100 °C of both the cellulosic and the ceramic papers are compared, it can be observed that the value corresponding to the ceramic paper (0.75 μmol/mg sample, Table 4) is higher than that of the cellulosic paper (0.46 μmol/mg sample). Nevertheless, the interaction of the hydrocarbon with both structures is low because when temperature increases, toluene does not remain retained.

On the other hand, the toluene adsorption capacity at 100 °C of "PCer Z" (Table 4) is slightly higher than that of "PCel Z" (Table 3). The calcination of the ceramic paper at 600 °C causes the cellulose destruction with the corresponding generation of holes and a more open structure is obtained. Thus, the higher adsorption capacity of the zeolitic ceramic paper could be related to a higher accessibility of the hydrocarbon towards the zeolitic adsorption sites.

4. Conclusions

Cellulosic papers were prepared, in which zeolite particles were retained by the addition of polymers. The NaY zeolite resulted homogeneously distributed and the zeolitic cellulosic papers were mechanically acceptable, which makes them promising for applications at low temperatures.

The combination of cellulosic pulp and ceramic fibers led to the obtention of ceramic papers. Zeolitic ceramic papers were prepared by the incorporation of NaY zeolite particles to the cellulose/ceramic matrix. Although a decrease in their mechanical properties due to calcination was observed, zeolitic ceramic papers resulted easy to handle for practical applications.

The prepared zeolitic papers resulted active as toluene sorbents, the adsorption capacities of zeolitic ceramic papers being higher. In the case of zeolitic cellulosic papers, the amounts of released toluene were lower than those of adsorbed toluene, implying that the treatment up to 160 °C did not completely eliminate the hydrocarbon. Also, TPD profiles showed that toluene is chemically retained up to high temperatures (ca. 420 °C) in zeolitic ceramic papers. This highlights the potential application of these zeolitic structures as sorbent materials for both low and high temperatures.

Appendix A. Supplementary material

Supplementary data associated with this article can be found, in the on-line version, at doi:10.1016/j.micromeso.2011.04.024.

References

[1] S. Aguado, A.C. Polo, M.P. Bernal, J. Coronas, J. Santamaría, J. Membr. Sci. 240 (1-2) (2004) 159–166.
[2] F.I. Khan, A.Kr. Ghoshal, J. Loss Prev. Process Ind. 13 (2000) 527–545.
[3] W.B. Li, J.X. Wang, H. Gong, Catal. Today 148 (2009) 81–87.
[4] H. Ichiura, T. Kitaoka, H. Tanaka, Chemosphere 50 (2003) 79–83.
[5] C.W. Kwong, Christopher Y.H. Chao, K.S. Hui, M.P. Wan, Atmos. Environ. 42 (2008) 2300–2311.
[6] C. Howard-Reed, S.J. Nabinger, S.J. Emmerich, Build. Environ. 43 (2008) 368–377.
[7] Yu. Matatov-Meytal, M. Sheintuch, Appl. Catal. A: General 231 (2002) 1–16.
[8] H. Ichiura, M. Nozaki, T. Kitaoka, H. Tanaka, Adv. Environ. Res. 7 (2003) 975–979.
[9] C.Y.H. Chao, C.W. Kwong, K.S. Hui, J. Hazard Mater. 143 (2007) 118–127.
[10] E.D. Banús, M.A. Ulla, M.V. Galván, M.A. Zanuttini, V.G. Milt, E.E. Miró, Catal. Commun. 12 (1) (2010) 46–49.
[11] SCAN Standard Methods SCAN-C 26:76 and SCAN-M 5:76.
[12] Y. Iguchi, H. Ichiura, T. Kitaoka, H. Tanaka, Chemosphere 53 (2003) 1193–1199.
[13] D. Vu, M. Marquez, G. Larsen, Micropor. Mesopor. Mater. 55 (2002) 93–101.
[14] H. Ichiura, Y. Kubota, Z. Wu, H. Tanaka, J. Mater. Sci. 36 (2001) 4921–4926.
[15] S. Soares, G. Camino, S. Levchik, Polym. Degrad. Stab. 49 (1995) 275–283.
[16] M.L.M. Olivera, A.A.L. Miranda, C.M.B.M. Barbosa, C.L. Cavalcante Jr., D.C.S. Azevedo, E. Rodriguez-Castellon, Fuel 88 (2009) 1885–1892.
[17] G. Leofanti, M. Padovan, G. Tozzola, B. Venturelli, Catal. Today 41 (1998) 207–219.
[18] R.M. Serra, E.E. Miró, M.K. Sapag, A.V. Boix, Micropor. Mesopor. Mater. 138 (2011) 102–109.
[19] A. Iliyas, M.H. Zahedi-Niaki, M. Eić, S. Kaliaguine, Micropor. Mesopor. Mater. 102 (2007) 171–177.